0022-3565/11/3362-313–320
THE JOURNAL OF PHARMACOLOGY AND EXPERIMENTAL THERAPEUTICS
U.S. Government work not protected by U.S. copyright
JPET 336:313–320, 2011

Vol. 336, No. 2
174904/3654793
Printed in U.S.A.

The Nitric Oxide Prodrug JS-K Is Effective against Non–Small-Cell Lung Cancer Cells In Vitro and In Vivo: Involvement of Reactive Oxygen Species[S]

Anna E. Maciag, Harinath Chakrapani,[1] Joseph E. Saavedra, Nicole L. Morris, Ryan J. Holland, Ken M. Kosak, Paul J. Shami, Lucy M. Anderson, and Larry K. Keefer

Basic Science Program (A.E.M., J.E.S.) and Laboratory Animal Sciences Program (N.L.M.), SAIC-Frederick, Inc., and Laboratory of Comparative Carcinogenesis (H.C., R.J.H., L.M.A., L.K.K.), National Cancer Institute, Frederick, Maryland; and Division of Medical Oncology, Huntsman Cancer Institute, University of Utah, Salt Lake City, Utah (K.M.K., P.J.S.)

Received September 8, 2010; accepted October 19, 2010

ABSTRACT

Non–small-cell lung cancer is among the most common and deadly forms of human malignancies. Early detection is unusual, and there are no curative therapies in most cases. Diazeniumdiolate-based nitric oxide (NO)-releasing prodrugs are a growing class of promising NO-based therapeutics. Here, we show that O^2-(2,4-dinitrophenyl)-1-[(4-ethoxycarbonyl)piperazin-1-yl]diazen-1-ium-1,2-diolate (JS-K) is a potent cytotoxic agent against a subset of human non–small-cell lung cancer cell lines both in vitro and as xenografts in mice. JS-K treatment led to 75% reduction in the growth of H1703 lung adenocarcinoma cells in vivo. Differences in sensitivity to JS-K in different lung cancer cell lines seem to be related to their endogenous levels of reactive oxygen species (ROS)/reactive nitrogen species (RNS). Other related factors, levels of peroxiredoxin 1 (PRX1) and 8-oxo-deoxyguanosine glycosylase (OGG1), also correlated with drug sensitivity. Treatment of the lung adenocarcinoma cells with JS-K resulted in oxidative/nitrosative stress in cells with high basal levels of ROS/RNS, which, combined with the arylating properties of the compound, was reflected in glutathione depletion and alteration in cellular redox potential, mitochondrial membrane permeabilization, and cytochrome *c* release. Inactivation of manganese superoxide dismutase by nitration was associated with increased superoxide and significant DNA damage. Apoptosis followed these events. Taken together, the data suggest that diazeniumdiolate-based NO-releasing prodrugs may have application as a personalized therapy for lung cancers characterized by high levels of ROS/RNS. PRX1 and OGG1 proteins, which can be easily measured, could function as biomarkers for identifying tumors sensitive to the therapy.

Introduction

Lung cancer is a leading cause of cancer deaths worldwide. Non–small-cell lung cancer (NSCLC) accounts for approximately 80% of all lung cancers. The disease is rarely curable, with an overall 5-year survival rate of only 15%. With current platinum-based chemotherapy regimens, median survival is 7 to 10 months for advanced disease (Schiller et al., 2002). It has become apparent that NSCLC is a heterogeneous disease, with many cellular and molecular changes potentially contributing to its development. Accordingly, emphasis has been shifting to targeting subsets of lung cancers based on specific cellular properties (Carbone, 2009).

Nitric oxide (NO) is a signaling molecule, a toxicant, and an antioxidant under various conditions, with a broad spectrum of actions in physiological and pathological processes. Both pro- and anti-cancer activities have been described,

This research was supported in part by the Intramural Research Program of the National Institutes of Health, National Cancer Institute, Center for Cancer Research, and the National Institutes of Health National Cancer Institute [Contract HHSN261200800001E].

[1] Current affiliation: Department of Chemistry, Indian Institute of Science Education and Research, Pune, India.

Article, publication date, and citation information can be found at http://jpet.aspetjournals.org.
doi:10.1124/jpet.110.174904.

[S] The online version of this article (available at http://jpet.aspetjournals.org) contains supplemental material.

ABBREVIATIONS: NSCLC, non–small-cell lung cancer; JS-K, O^2-(2,4-dinitrophenyl)-1-[(4-ethoxycarbonyl)piperazin-1-yl]diazen-1-ium-1,2-diolate; ROS, reactive oxygen species; RNS, reactive nitrogen species; PRX, peroxiredoxin; OGG1, 8-oxo-deoxyguanosine glycosylase; BER, base excision repair; MnSOD, manganese superoxide dismutase; MTT, (3-(4,5-dimethylthiazol-2-yl)-2,5-diphenyltetrazolium bromide; HBSS, Hank's balanced salt solution; PARP, poly(ADP-ribose) polymerase; IL, interleukin; DMSO, dimethyl sulfoxide; PBS, phosphate-buffered saline; DCF, 2′,7′-dichlorofluorescein; DAF-FM, 4-amino-5-methylamino-2′,7′ difluorofluorescein; GSSG, glutathione disulfide; NAC, *N*-acetylcysteine; BSO, buthionine sulfoximine; siRNA, small interfering RNA; JS-43-126, 1-(2,4-dinitrophenyl)-4-carboethoxypiperazine; 8-oxodG, 8-oxo-7,8-dihydro-2′-deoxyguanosine.

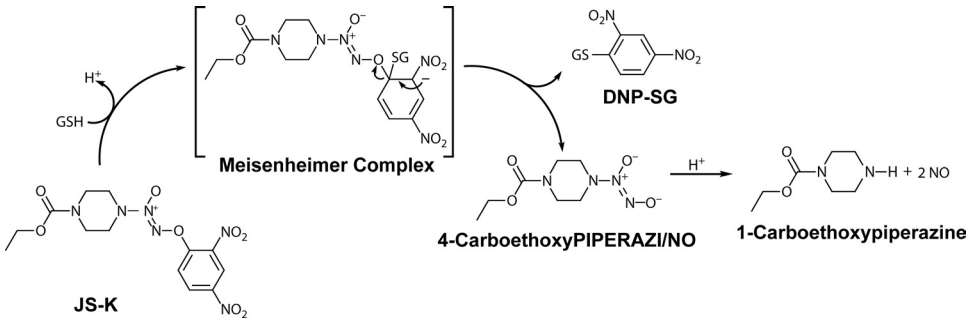

Fig. 1. Structure of JS-K and scheme of nitric oxide release upon reaction with GSH. DNP-SG, *S*-(2,4-dinitrophenyl)glutathione.

depending on cell type and conditions, the source of NO, its concentration, rate of release, and other factors (Kröncke et al., 1997; Hofseth et al., 2003; Pacher et al., 2007). NO donor drugs have induced apoptosis in several types of human cancer cells (Bonavida et al., 2006, 2008; Huerta et al., 2008), including prostate (Royle et al., 2004) and colon (Jarry et al., 2004). In general, the concentrations required have suggested limited clinical applicability. In contrast, the diazeniumdiolate-based NO-donor prodrug, O^2-(2,4-dinitrophenyl)-1-[(4-ethoxycarbonyl)piperazin-1-yl]diazen-1-ium-1,2-diolate (JS-K) (Fig. 1), is highly cytotoxic to leukemia and multiple myeloma cell lines and patient-derived multiple myeloma cells, with IC_{50} values ranging from 0.2 to 1.2 μM (Shami et al., 2003; Kiziltepe et al., 2007). It is noteworthy that JS-K was selectively cytotoxic toward cancer cells. At concentrations at which it inhibited the proliferation of multiple myeloma cells, JS-K had no significant toxicity toward normal peripheral blood mononuclear cells or bone marrow stromal cells (Kiziltepe et al., 2007).

Other types of cancer cells were also effectively killed by JS-K, including prostate cancer (Shami et al., 2003) and hepatoma cells (Ren et al., 2003). A survey of the National Cancer Institute panel of 51 cancer cell lines suggested sensitivity of renal cancers, and correspondingly we found approximately 10-fold selectivity observed for renal cancer cells compared with noncancerous renal epithelial cells (Chakrapani et al., 2008). Only moderate effects were observed for the several lung cancer cell lines in the National Cancer Institute panel. However, in view of the cellular heterogeneity among lung cancers, we surveyed a larger panel of 18 lung adenocarcinoma cell lines and found that a subset of six lines is as susceptible to killing by JS-K as leukemia and multiple myeloma cells, with IC_{50} values in the range of 0.33 to 1.01 μM. Cell effects include alterations in cellular redox potential, marked DNA strand break damage, and mitochondrially mediated apoptosis. Reasons for the high sensitivity of this subset of NSCLC cells were sought. The IC_{50} values show strong correlations with intracellular reactive oxygen species (ROS)/reactive nitrogen species (RNS) (negative) and with levels of 8-oxoguanine glycosylase (OGG1) protein, a repair enzyme for oxidative DNA damage (positive). Both ROS level and IC_{50} values for JS-K correlate strongly with levels of peroxiredoxin 1 (PRX1) protein. OGG1 and PRX1 protein levels may be convenient biomarkers for identification of subsets of lung cancers with potential therapeutic responsiveness to JS-K.

Materials and Methods

JS-K Synthesis and Chemicals. JS-K was synthesized as described previously (Saavedra et al., 2001). All other chemicals were obtained from Sigma-Aldrich (St. Louis, MO). siRNA to six isoforms of PRX was obtained from Santa Cruz Biotechnology, Inc. (Santa Cruz, CA). HiPerfect transfection reagent and AllStars nonsilencing siRNA control were from QIAGEN (Valencia, CA).

Cell Culture and Proliferation Assay. Cell lines were obtained from the American Type Culture Collection (Manassas, VA) and cultured according to the supplier's protocol. For proliferation assays cells were seeded at 2×10^4 per well in 96-well plates and allowed to adhere for 24 h. JS-K was prepared as 10 mM stock solution in DMSO. Increasing drug concentrations in 10 μl of PBS were added to 100 μl of the culture medium for 48 h. MTT assay (Promega, Madison, WI) was performed according to the manufacturer's protocol. Each concentration was represented in six repeats, and the screening was performed as at least two independent experiments. IC_{50} values were calculated by using Sigma Plot software (Systat Software, Inc., San Jose, CA).

In Vivo Treatments. All animals used in this research project were cared for and used humanely according to the following policies: the U.S. Public Health Service Policy on Humane Care and Use of Animals (1996), the National Institutes of Health's *Guide for the Care and Use of Laboratory Animals* (1996), and the U.S. Government Principles for Utilization and Care of Vertebrate Animals Used in Testing, Research, and Training (1985). All National Cancer Institute-Frederick animal facilities and the animal program are accredited by the Association for Assessment and Accreditation of Laboratory Animal Care International. H1944 or H1703 cells were injected at 5×10^6 s.c. into a flank of 7-week-old female athymic NCr-nu/nu mice (Charles River Laboratories, Inc., Wilmington, MA). The drug injections were initiated when the tumors reached $2 \times 2 \times 2$ mm (typically 3–4 weeks). JS-K was formulated in Pluronic P123 (BASF, Florham Park, NJ) micelles. Animals were treated three times a week for 3 weeks with intravenous tail vein injections of either vehicle (2.25% Pluronic P123 in PBS) or JS-K (6 μmol/kg in the vehicle). Tumors were measured with a caliper twice a week, and the tumor volumes were calculated by using a formula for ellipsoid volume, $\pi/6 \times$ length $\times$ width $\times$ height (Tomayko and Reynolds, 1989). The nonparametric Mann-Whitney test was used for statistical comparisons of tumor volumes at each time point. Body weights were taken before each drug injection. Animals were sacrificed 2 h after the last drug injection. Blood was collected by cardiac puncture under isoflurane anesthesia for testing for cytokines. Cytokines in serum were measured by using a mouse Th1/2 multiplex assay (Meso Scale Discovery, Gaithersburg, MD), according to the manufacturer's protocol. There were 9 to 13 mice/group at termination.

Determination of Intracellular Reactive Oxygen/Nitrogen Species and Nitric Oxide. Intracellular level of reactive oxygen/nitrogen species was quantified by the oxidation of the ROS/RNS-sensitive fluorophore 5-(and-6)-chloromethyl-2′,7′-dichlorodihydrofluorescein diacetate (Invitrogen, Carlsbad, CA). Cells growing on six-well plates (6×10^5/well) were loaded with 5 μM 5-(and-6)-chloromethyl-2′,7′-dichlorodihydrofluorescein diacetate in Hanks' balanced salt solution (HBSS) at 37°C and 5% CO_2. After 30 min of incubation, HBSS containing the probe was removed, cells were rinsed with HBSS, and 3 ml of fresh HBSS was added to each well followed by addition of JS-K or DMSO as a control. After 30 or 60 min

the cells were collected by scraping in HBSS, and 2′,7′-dichlorofluorescein (DCF) fluorescence was measured by using a PerkinElmer Life and Analytical Sciences (Waltham, MA) LS50B luminescence spectrometer with the excitation source at 488 nm and emission at 530 nm.

The intracellular level of nitric oxide after JS-K treatment was quantified by using the NO-sensitive fluorophore 4-amino-5-methylamino-2′,7′ difluorofluorescein (DAF-FM) diacetate (Invitrogen). Cells growing on six-well plates were loaded with 2.5 μM DAF-FM diacetate in HBSS at 37°C and 5% CO_2. After 30 min of incubation the cells were rinsed with HBSS to remove excess probe, and JS-K in fresh HBSS was added to the cells at 1 μM final concentration. After 30- or 60-min incubation the fluorescence of the benzotriazole derivative formed on DAF-FM's reaction with aerobic NO was analyzed by using a PerkinElmer Life and Analytical Sciences LS50B luminescence spectrometer with the excitation source at 495 nm and emission at 515 nm.

All experiments were performed at least three times, each time in triplicate.

Immunoblotting. Mitochondrial and cytosolic fractions were prepared by subcellular fractionation. The cells (20×10^6) were collected with trypsin, rinsed with cold PBS, and resuspended in 400 μl of hypotonic buffer [10 mM Tris-HCl, pH 7.5 containing 10 mM NaCl, 1.5 mM $MgCl_2$, 1 mM phenylmethylsulfonyl fluoride, and Complete protease inhibitors cocktail (Roche Diagnostics, Indianapolis, IN)]. Cells were incubated on ice for 10 min and homogenized by using a Dounce homogenizer with a B pestle. A volume of 500 μl of mitochondrial buffer (12.5 mM Tris-HCl, pH 7.5 containing 525 mM mannitol, 175 mM sucrose, 2.5 mM EDTA, and protease inhibitors) was added to the resulting homogenate, and the mixture was centrifuged twice at 1300*g* for 5 min at 4°C. The resulting supernatant was centrifuged at 10,000*g* for 10 min at 4°C. The supernatant (cytosolic fraction) was collected. The pellet (mitochondrial fraction) was resuspended in hypotonic buffer containing 0.5% Triton X-100 and rotated for 30 min at 4°C.

For immunoprecipitation 300 μg of the cell lysate was incubated on the rotator overnight at 4°C with 2 μg of anti-nitrotyrosine monoclonal antibody and 30 μl of protein G agarose. After washing three times with lysis buffer the beads were suspended in 30 μl of 2× NuPAGE (Invitrogen) loading buffer and heated for 10 min at 95°C. Immunoprecipitated material was resolved on SDS-polyacrylamide gel electrophoresis followed by immunoblotting with anti-MnSOD antibody.

For cytochrome *c* release, H1703 cells were seeded at 2×10^6 onto 10-cm Petri dishes and allowed to grow for 24 h. JS-K was added to the medium to a final concentration 1 or 10 μM. Cells were rinsed three times with ice-cold PBS and digitonin [200 μl of 190 μg/ml in lysis buffer (PBS containing 75 mM KCl, 250 mM sucrose and Complete protease inhibitors cocktail (Roche Diagnostics)] was added for 10 min on ice. Cells were then scraped gently and centrifuged 10 min at 12,000*g* at 4°C. The supernatant (cytosolic fraction) was removed, and the remaining pellet (mitochondrial fraction) was resuspended in 100 μl of lysis buffer (25 mM HEPES buffer containing 150 mM NaCl, 10 mM $MgCl_2$, 1% Nonidet P40, 0.25% sodium deoxycholate, 10% glycerol, 2.5 mM EDTA, and Complete protease inhibitors cocktail) and allowed to incubate for 30 min.

Western blot analysis was performed as described previously (Romanowska et al., 2007). Primary antibodies for caspase 3, caspase 7, PARP, cleaved PARP, Bax, cytochrome *c* (Cell Signaling Technology, Danvers, MA), PRX 1 to 6 (LabFrontier, Seoul, Korea), and nitrotyrosine and MnSOD (Millipore Corporation, Billerica, MA) were used.

Mitochondrial Superoxide Measurement. Mitochondrial superoxide level was measured by using MitoSOX fluorescent dye (Invitrogen), according to the manufacturer's protocol. Rotenone (10 μM) was used as a positive control.

Measurement of Cellular Glutathione Content. H1703 or H1944 cells were plated in six-well plates at 6×10^5 per well. Cells were treated with JS-K for 1 h at 1 μM (H1703 cells) or 10 μM (H1944 cells). After treatment, cells were washed with PBS, scraped into PBS, and collected by centrifugation at 800*g* for 10 min. The pellets were resuspended in 80 μl of 10 mM HCl and lysed by two successive rounds of freeze and thawing. Twenty microliters of a 5% 5-sulfosalicylic acid solution was added to the lysate. The precipitate was removed by centrifugation at 8000*g* for 10 min, and the supernatant was analyzed for total GSH content by using a total glutathione quantification kit (Dojindo, Rockville, MD) according to the manufacturer's protocol. To measure glutathione disulfide (GSSG) concentration, cells were treated and lysed in accordance with the procedure above. The lysate was then neutralized with 0.1 M NaOH and treated with 4-vinylpyridine at a final concentration of 50 mM for 30 min.

Measurement of Mitochondrial Membrane Potential. H1703 cells were seeded on 24-well plates at 2×10^5/well and allowed to grow for 24 h. The cells were then treated with either vehicle (DMSO) or 1 to 10 μM JS-K and incubated at 37°C, 5% CO_2 for 30 min. The JC-1 Mitochondrial Membrane Potential Assay Kit (Cayman Chemical, Ann Arbor, MI) was used according to the manufacturer's protocol.

Comet Assay. The alkaline comet assay was performed as described previously (Romanowska et al., 2007).

Statistical Analysis. All experiments (with the exception of the proliferation assay) were performed at least three times, each time at least in triplicate. Results are presented as averages ± S.E. Statistical tests were carried out by using Instat version 3.00 (GraphPad Software Inc., San Diego, CA). Pairwise comparisons included the *t* test, with the Welch correction or application of the Mann-Whitney test as appropriate. Significance of correlations was assessed by the Pearson linear correlation or the Spearman test as appropriate.

Results

JS-K Has a Strong Inhibitory Effect on a Subset of Human NSCLC Cells in Culture and an In Vivo Xenograft Model. JS-K inhibited growth of all NSCLC cell lines with IC_{50} concentrations ranging from 0.33 to 17.64 μM (Table 1). Six cell lines were inhibited by JS-K in the range of 0.33 to 1.01 μM and were thus as sensitive as leukemia cells (Shami et al., 2003, 2006) or multiple myeloma cells (Kiziltepe et al., 2007). Sensitive H1703 cells and resistant H1944

TABLE 1

NSCLC cell lines used in the study, IC_{50} values for JS-K, and some of the cell lines' characteristics

IC_{50} values were obtained from 10 concentrations over the range 50 nM to 50 μM, with six replicates for each cell line. NCI, National Cancer Institute; ATCC, American Type Culture Collection.

Designation NCI//ATCC	JS-K IC_{50}	K-ras	p53
	μ*M*		
H1693/CRL5887	0.33	WT	WT
H1734/CRL5891	0.36	c13 TGC	mut c273 high
H1568/CRL5876	0.40	WT	WT
H1703/CRL5889	0.40	WT	mut c285
H1373/CRL5866	0.97	c12 TGT	mut c47
H441/HTB174	1.01	c12 GTT	mut c158 low
H1395/CRL5868	3.17	WT	x
H2126/CRL5925	4.13	WT	WT
H838/CRL5844	5.84	WT	WT
H2122/CRL5985	6.09	c12 TGT	x
A549/CCL185	7.60	c12 AGT homozygous	WT
H460/HTB177	7.61	c61 CAT	WT
H1355/CRL5865	7.93	c13 TGC	mut c285 low
H322/CRL5806	8.71	WT	mut c248 high
H1792/CRL5895	9.08	c12 TGT	mut, splice
H2023/CRL5912	11.55	WT	WT
H2030/CRL5914	14.74	c12 TGT	WT
H1944/CRL5907	17.64	c13 GAC	WT

WT, wild type; c, codon with mutation; x, not reported.

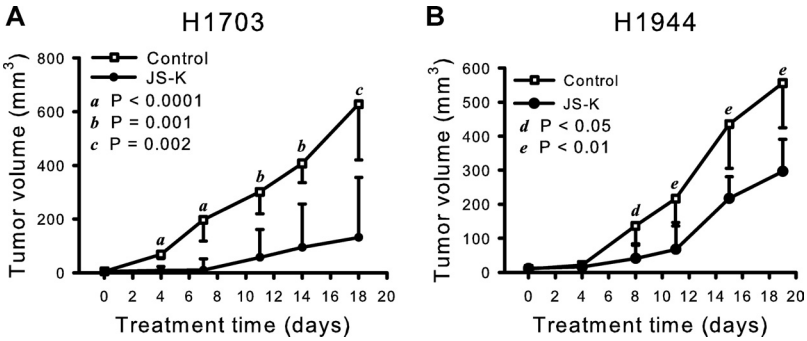

Fig. 2. JS-K significantly reduced growth of NSCLC cells in vivo. JS-K was administered intravenously at 6 μmol/kg, three times a week for 3 weeks, and tumors were measured with a caliper. Growth of both cell lines, JS-K-sensitive H1703 (A) and over 10-fold less sensitive H1944 (B), was inhibited. Values are medians, and the relevant 95% confidence interval bars are shown (Mann-Whitney test). Letters indicate the significance of the differences between JS-K-treated and control mice at each time point. The treatment did not affect body weights. The average body weight for all mice was 22.7 ± 0.25 g (mean ± S.E.) at the beginning of the experiment. At the termination, the average weights of the control groups were 24.57 ± 0.88 g (n = 11) and 24.41 ± 0.57 g (n = 13), for H1703 and H1944 xenograft studies, respectively. The weights of JS-K treated animals were 24.92 ± 0.39 g (n = 9) and 24.42 ± 0.56 g (n = 11), for the H1703 and H1944 xenograft groups, respectively.

cells were chosen for assessment of activity of JS-K in vivo against xenografted tumor cells in athymic mice. These cell lines have very similar doubling times. JS-K significantly reduced growth of both H1703 and H1944 human NSCLC cells compared with cells in control animals treated with vehicle only (Fig. 2). The growth inhibition was much more pronounced for H1703 xenografts than for H1944 cells, as predicted from the cell culture results (Table 1), although H1944 cells growth in vivo was also significantly inhibited (Fig. 2B). It is noteworthy that the treatment with either vehicle or JS-K did not affect body weight (see legend to Fig. 2). Serum samples collected from the animals at termination were tested for levels of cytokines. There were no significant differences in levels of IL-1β, IL-2, IL-4, IL-5, IL-10, IL-12, interferon-γ, or tumor necrosis factor-α between the JS-K-treated and control groups.

JS-K Effectiveness in Inhibiting Lung Cancer Cells' Growth Correlated with Intracellular ROS/RNS Level. We sought to determine the reasons behind the differences in sensitivity to JS-K between the cell lines. Information is available regarding the origin and cancer genes mutational status of some of the cell lines used (Phelps et al., 1996; Romanowska et al., 2007) (Table 1). There was no obvious association between JS-K toxicity and mutational status of *p53* or *K-ras*. The cell lines had previously been characterized by us with regard to levels of ROS (Romanowska et al., 2007). Inspection of the assembled data suggested that JS-K was most effective against cell lines characterized by high levels of ROS, as detected by the oxidation-sensitive fluorophore DCF. It should be noted that this fluorophore is also oxidized by RNS such as peroxynitrite (Halliwell and Whiteman, 2004). There was a strong and statistically significant correlation between endogenous ROS/RNS (DCF fluorescence) and JS-K toxicity, measured as IC_{50} values (P = 0.0004, r = −0.75; Fig. 3A). IC_{50} values did not correlate significantly with total levels of superoxide as measured by nitroblue tetrazolium reduction (Romanowska et al., 2007) (Supplementary Fig. S1).

To confirm a controlling role for ROS/RNS in lung cancer cells' susceptibility to JS-K, we demonstrated that the antioxidant *N*-acetylcysteine (NAC) abrogated the effect of JS-K in the drug-sensitive H1703 cell line (Fig. 3B). Buthionine sulfoximine (BSO), a pro-oxidant via GSH depletion, increased effectiveness of JS-K in a dose-dependent way in H1703 cells (Fig. 3B). BSO also potentiated the JS-K effect in the less sensitive H1944 cells (Fig. 3C).

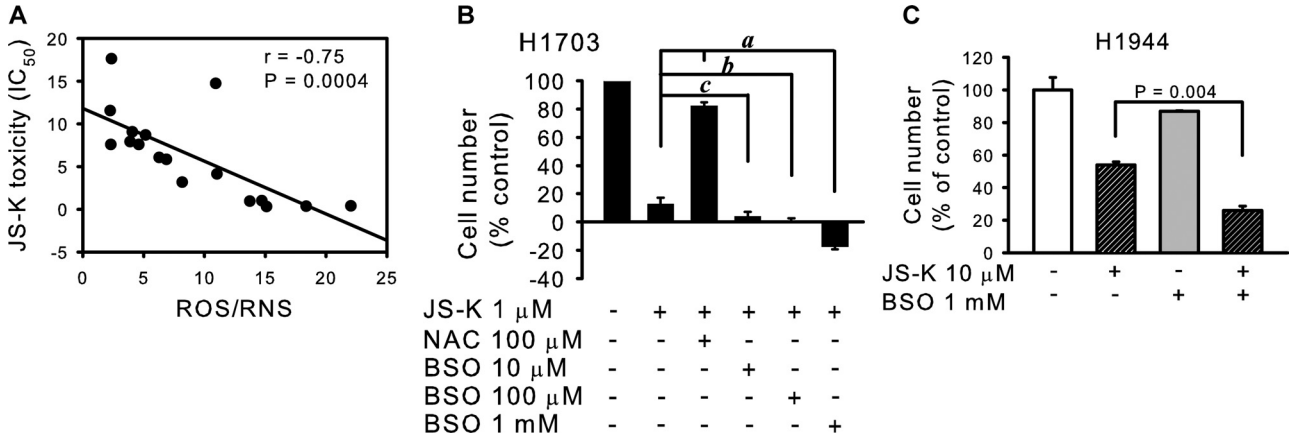

Fig. 3. JS-K toxicity depends on intracellular ROS/RNS. A, JS-K toxicity (as IC_{50} values) correlated significantly with endogenous ROS/RNS levels, measured as DCF fluorescence (arbitrary units). B, pretreatment with NAC reduced JS-K toxicity, whereas depletion of glutathione using the glutathione synthase inhibitor BSO sensitized the cells to JS-K. The H1703 cells were treated with NAC or BSO for 24 h, followed by 24 h with 1 μM JS-K. The number of surviving cells was assessed by the MTT assay. a, $P < 0.0001$; b, $P = 0.003$; c, $P = 0.04$ by Mann-Whitney test. C, depletion of GSH in the H1944 cells sensitized the cells to JS-K. Cells were treated with 1 mM BSO in complete medium for 24 h followed by 10 μM JS-K for another 24 h, and the number of surviving cells was assessed by the MTT assay.

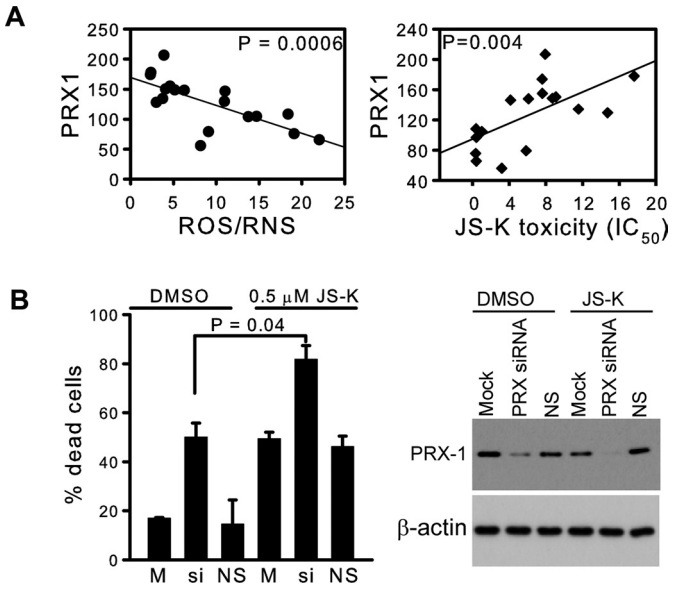

Fig. 4. A, protein levels of PRX1 (expressed relative to the HPL1D cell line used as an internal control) correlated negatively with intracellular ROS/RNS level measured as DCF fluorescence (arbitrary units). JS-K toxicity measured as IC_{50} values correlated with levels of PRX1. B, silencing of peroxiredoxins with a pool of siRNAs sensitized the cells to JS-K. H1703 cells were treated with a siRNA pool for all six isoforms of PRX for 48 h in complete medium followed by 0.5 μM JS-K for 24 h. Percentage of dead cells was measured by the trypan blue exclusion method. Loss of PRX-1 signal after siRNA treatment was shown by Western blot. M, mock control; si, siRNA to PRX pool; NS, nonsilencing siRNA negative control.

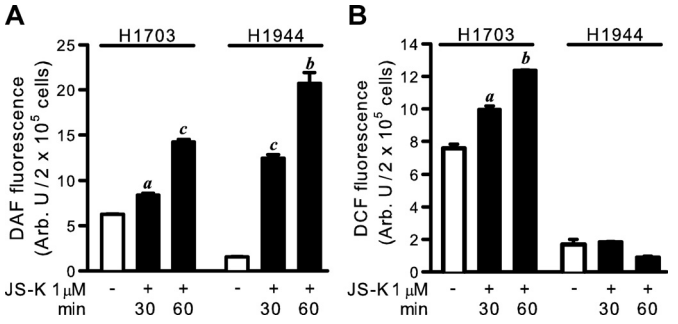

Fig. 5. A, intracellular NO release after JS-K treatment measured as DAF fluorescence. B, intracellular ROS/RNS level after JS-K treatment measured as DCF fluorescence. A representative experiment is shown ($n = 4$). a, $P < 0.01$; b, $P < 0.001$; c, $P < 0.0001$, by paired t test, compared with cells treated with DMSO only.

Several antioxidant enzymes may contribute to the regulation of steady-state levels of ROS in cells. In our panel of NSCLC cells, ROS/RNS did not correlate with levels of MnSOD, CuZn superoxide dismutase, catalase, glutathione peroxidase, or PRX2 and PRX5 (not shown). However, there was a significant negative correlation of ROS/RNS with PRX 1, 3, 4, and 6 (Fig. 4A and Supplementary Fig. S2), supporting the importance of these enzymes in the antioxidant defense system of lung cancer cells. In addition to their action on peroxides, PRXs are recognized as highly efficient peroxynitrite scavengers (Ferrer-Sueta and Radi, 2009). Protein levels of PRX1 had a strong negative correlation with ROS/RNS and a strong positive correlation with the IC_{50} values for JS-K (Fig. 4A). There was a similar, although less pronounced, correlation with PRX6 (Supplementary Figs. S2 and S3). Down-regulation of the PRXs with a pool of siRNAs resulted in a significant increase in cell killing by 0.5 μM JS-K (Fig. 4B). There were no significant correlations between JS-K IC_{50} values and levels of catalase, CuZn superoxide dismutase, MnSOD, or glutathione peroxidase (not shown). These results confirm the pivotal role of ROS/RNS level in determination of lung cancer cell sensitivity to killing by JS-K and suggest that expression of PRX1 protein might be a useful clinical indicator.

Increase in NO and ROS/RNS after JS-K. To confirm that JS-K released NO in the cells, an increase in intracellular NO was demonstrated up to 60 min after treatment with the NO-specific reagent DAF-FM diacetate and occurred in both the sensitive H1703 and the resistant H1944 cell lines (Fig. 5A). There was also an increase in DCF-reactive material over this time frame in H1703 cells, but not H1944 cells (Fig. 5B), suggesting that pre-existing high levels of ROS/RNS were required for the generation of additional ROS/RNS.

Effects of JS-K on Mitochondria and Glutathione Oxidation. The increased ROS/RNS in H1703 cells suggested occurrence of the well known uncoupling effects of NO in mitochondria, resulting in increased superoxide, hydrogen peroxide, and peroxynitrite. There was correspondingly an increase in mitochondrial superoxide generation in the cells (Fig. 6A). NO might also increase levels of superoxide and peroxynitrite by inhibition of mitochondrial MnSOD. The enzyme has three tyrosine residues susceptible to nitration (Tyr45, Tyr193, and Tyr34); Tyr34 is critical for activity. Nitration of the active-site residue Tyr34 of MnSOD results

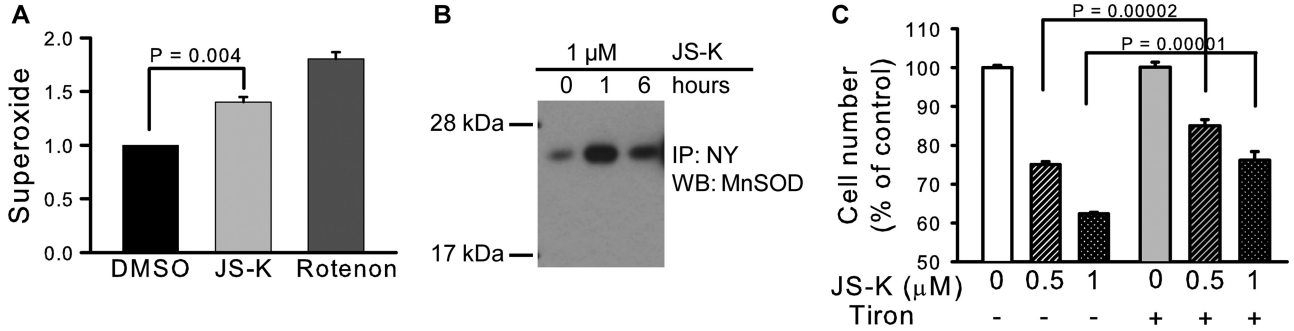

Fig. 6. JS-K-induced increase in mitochondrial superoxide and MnSOD tyrosine nitration. A, mitochondrial superoxide level measured with MitoSOX fluorescence. Rotenone was used as positive control. B, H1703 cells were treated with 1 μM JS-K for 1 or 6 h. The level of 3-nitrotyrosine (NY) in MnSOD was assessed by immunoprecipitation (IP) with an anti-nitrotyrosine antibody followed by immunoblot (WB) with an antibody to MnSOD. C, the superoxide scavenger Tiron had a protective effect against JS-K toxicity; H1703 cells were pretreated with 10 mM Tiron in complete medium for 1 h, followed by 24 h with JS-K and then the cell number was assessed by MTT assay.

TABLE 2
Changes in glutathione homeostasis in NSCLC cells upon JS-K treatment
Results of one experiment representative of three are shown.

	GSH	GSSG	GSH/GSSG
	μmol/mg protein		
H1703			
DMSO	1.55	0.028	55.4
JS-K 1 μM	1.27	0.042	30.2
H1944			
DMSO	0.25	0.008	31.3
JS-K 10 μM	0.13	0.014	9.3

in nearly complete inhibition of catalysis (MacMillan-Crow et al., 1998; Yamakura et al., 1998). A significant increase in the nitrotyrosine level in MnSOD was detected by immunoprecipitation in H1703 cells after 1 h with JS-K (Fig. 6B). Involvement of superoxide was also shown by using a superoxide scavenger Tiron, which had a protective effect against JS-K toxicity in the H1703 cell line (Fig. 6C).

These effects in the mitochondria suggested the likelihood of an overall change in the redox balance in the H1703 cells, and this was confirmed by a decrease in reduced GSH level and increase in its oxidized (GSSG) form (Table 2). In addition to indirect effects mediated via mitochondrial actions, JS-K may have a direct depleting effect on GSH. JS-K is activated to release NO by nucleophilic aromatic substitution of GSH at the aryl group, leading to Meisenheimer complex formation, and this reaction can be accelerated by glutathione transferases (Fig. 1) (Shami et al., 2003). Thus JS-K treatment should lead to GSH depletion both by this S_NAr reaction and through GSH oxidation by the observed increase in ROS/RNS (Fig. 5B). JS-K treatment reduced levels of GSH and increased levels of GSSG in the resistant cell line H1944 as well (Table 2). Untreated H1703 cells have more GSH than H1944 cells. This could favor JS-K toxicity in two ways: JS-K may be more effectively cleaved in the cells containing higher levels of GSH, and kinetic studies indicated that high GSH may in fact favor apoptosis because of its reaction with antiapoptotic species (Bagci et al., 2008).

Toxicity of JS-K in Sensitive Cells Is Associated with Induction of the Intrinsic Apoptotic Pathway. GSH depletion leading to redox imbalance, as demonstrated above, may activate the intrinsic apoptotic pathway initiator Bax by its oxidation-dependent dimerization and consequent translocation to mitochondria (D'Alessio et al., 2005). This functional translocation triggers cytochrome *c* release from mitochondria, which makes Bax translocation the most upstream event of the intrinsic apoptotic pathway. The two cysteine residues of Bax form a disulfide bridge, which changes the conformation of the protein to that favorable for mitochondrial translocation (D'Alessio et al., 2005). In our sensitive H1703 cells, there were increases in total Bax and Bax dimers in the mitochondrial fraction within 20 min after treatment with 1 μM JS-K (Fig. 7B). Loss of mitochondrial membrane potential was detected after 1-h incubation with 1 μM JS-K; there was marked loss of this membrane potential with 10 μM JS-K (Fig. 7A). Cytochrome *c* release into the cytosol was detected 1 h after JS-K treatment was initiated (Fig. 7C). Apoptosis was activated early, as evidenced by cleaved caspases 3 and 7 (1 h), and cleaved PARP (1 h) (Fig. 7D). These effectors of apoptosis were not seen in the resistant H1944 cells, even at a 10-fold higher dose of JS-K (Fig. 7D). In H1944 cells 8-h treatment with 10 μM JS-K did not activate apoptosis (Fig. 7D) and 24-h treatment led only to a weak apoptotic response, as indicated by PARP and caspase 7 cleavage (Fig. 7E). However, pretreatment of H1944 cells with 1 mM BSO for 16 h followed by JS-K treatment for 24 h resulted in a strong apoptotic signal (Fig. 7E), confirming the likely involvement of pre-existing oxidative stress in initiating of apoptosis.

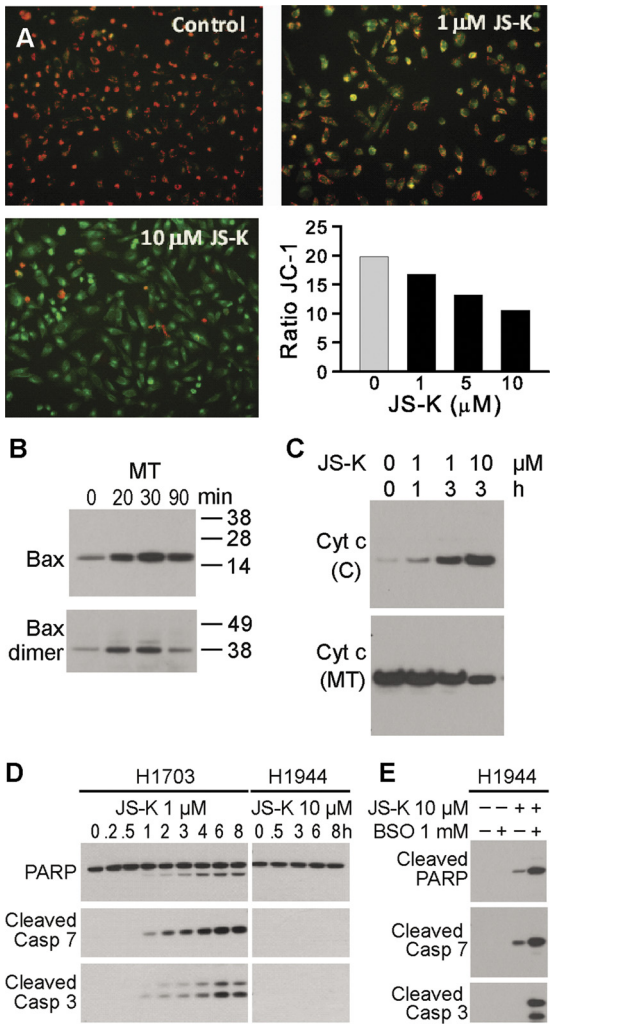

Fig. 7. A, mitochondrial membrane potential (ΔΨm) was analyzed using JC-1 mitochondrial membrane dye. H1703 cells were treated with DMSO (control) or JS-K (1–10 μM) for 1 h. The drug caused an increase in the green (JC-1 monomers) and decrease in the red fluorescence (JC-1 aggregates) indicative of loss of ΔΨm. Ratio of JC-1 (red to green) was calculated. B, immunoblot demonstrating increase in total Bax and Bax dimers in mitochondrial fraction (MT) within 20 min after 1 μM JS-K treatment. C, cytochrome *c* increase in the cytosol (C) and decrease in the mitochondria (MT) of H1703 cells after JS-K treatment. D, PARP cleavage and effector caspase 3 and 7 activation as shown by Western blot, in the H1703 cells, but not in JS-K-resistant H1944 cells, even at a 10-fold higher concentration of the drug. E, pretreatment with pro-oxidant BSO for 16 h sensitized H1944 cells for apoptosis after 24 h treatment with JS-K.

DNA Damage Contributed to JS-K's Toxicity. We noted previously in the NSCLC cell line panel a correlation between DNA strand break damage as assessed by the comet assay and the levels of superoxide. Baseline levels of total superoxide were low in H1703 cells compared with other lines, as indicated by the nitroblue tetrazolium assay (Romanowska et al., 2007). Correspondingly, the increase in

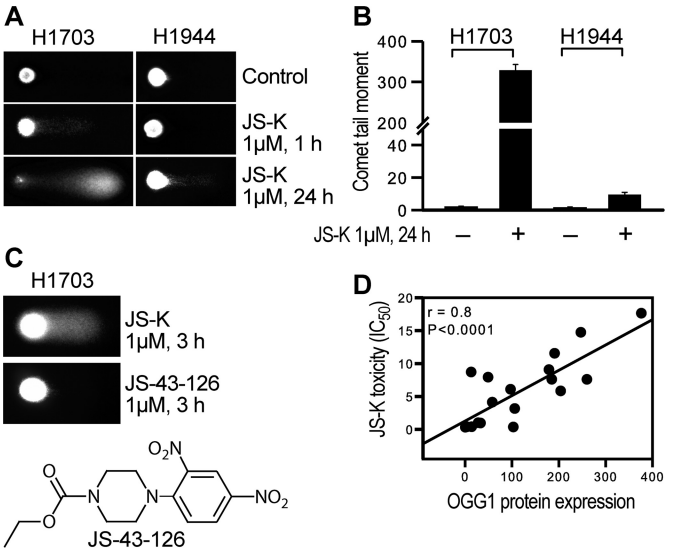

Fig. 8. DNA strand break damage analyzed by comet assay. A, comparison of comet signals in H1703 and H1944 cells after JS-K treatment. B, comet tail moment was quantified using CometScore software (TriTek Inc., Sumerduck, VA). C, JS-43-126, a non-NO-releasing JS-K analog (seen in the scheme), did not cause DNA strand break damage. D, OGG1 levels correlated significantly with JS-K toxicity measured as IC_{50} value.

mitochondrial superoxide in H1703 cells after JS-K treatment (Fig. 6A) was associated with extensive DNA damage within 1 h, with no effect seen in the resistant H1944 cell line (Fig. 8A). By 24 h massive damage was apparent in H1703 cells (Fig. 8, A and B). 1-(2,4-Dinitrophenyl)-4-carboethoxypiperazine (JS-43-126), an analog of JS-K that does not release NO, did not cause DNA strand break damage (Fig. 8C).

A major product of ROS attack in genomic DNA is the premutagenic lesion 8-oxo-7,8-dihydro-2′-deoxyguanosine (8-oxodG). The main defense against the 8-oxodG is the base excision repair (BER) pathway, which in eukaryotes is initiated by the OGG1 protein, a DNA glycosylase that catalyzes the excision of 8-oxodG from DNA, and is responsible for more than 95% of the BER activity in mammalian cells. In the present work we found a strong and statistically significant correlation between OGG1 protein expression levels and IC_{50} values for JS-K ($r = 0.8$, $P = 0.0001$; Fig. 8D). JS-K was much less toxic in the cell lines expressing high levels of OGG1 protein. These results confirm that DNA damage was part of the mechanism of JS-K's effects on the lung cancer cells and establish OGG1 as a potential marker for sensitivity. The strong association between OGG1 and the cell-killing effects of JS-K in the panel of cells clearly implicates oxidative DNA damage as a critical component. Activation of apoptosis by DNA damage frequently involves activation of p53. However, H1703 cells express only low levels of mutant inactive p53 (Phelps et al., 1996), and as expected no alterations in p53 levels or phosphorylation were observed after JS-K treatment; p73 was expressed at low levels but also was not altered (not shown).

Discussion

Lung cancer is rarely curable, despite the advances in understanding molecular mechanisms of cancer and new anticancer drug development. Novel therapeutic strategies are critically needed. In this article, we demonstrate that the diazeniumdiolate-based nitric oxide-releasing prodrug JS-K is highly effective against a third of the non–small-cell lung cancer cell lines studied here and is also active in vivo. The effectiveness of the drug is significantly correlated with preexisting high levels of ROS/RNS. Many cancer cell types, especially in advanced stage tumors, exhibit increased levels of ROS (Pelicano et al., 2004; Trachootham et al., 2009), and these high-ROS cells are likely to be more vulnerable to damage by further ROS/RNS released from an exogenous source than nonmalignant cells. In the present work, we show that 30% of the lung adenocarcinoma cell lines studied are characterized by high levels of ROS/RNS and are highly sensitive to JS-K. The drug was significantly effective in mouse xenograft models of lung adenocarcinoma without toxicity to the animals, suggesting potential clinical therapeutic efficacy. The selectivity of JS-K toward cancer cells while sparing nontransformed cells has been demonstrated previously (Shami et al., 2003; Kiziltepe et al., 2007; Chakrapani et al., 2008). Activity of candidate drugs in lung cancer xenografts has previously predicted clinical efficacy (Voskoglou-Nomikos et al., 2003). Thus, JS-K is a new agent that might have potential in the treatment of NSCLC. The cytotoxic effects of JS-K involved activation of the intrinsic apoptotic pathway. Inhibitory tyrosine nitration of mitochondrial MnSOD and increased mitochondrial superoxide were demonstrated, as well as increase in the DCF signal that could measure peroxides and/or peroxynitrite. It seems likely that these changes reflect the well known uncoupling effects of NO in mitochondria, caused by inhibition of cytochrome *c* oxidase (Brookes et al., 1999; Shiva et al., 2001; Brown and Borutaite, 2006; Bonavida et al., 2006). A low concentration (1 μM) of an NO-releasing chemical caused a marked increase in DCF signal in both cells and isolated mitochondria (Borutaite and Brown, 2003). Inhibition of catalase at low NO levels is also possible (Brown and Borutaite, 2006; Rauen et al., 2007). Engagement of the intrinsic mitochondrial pathway is typical for NO-induced apoptosis (Li and Wogan, 2005; Pacher et al., 2007). Direct toxic effects on mitochondrial membranes may have contributed to cytochrome *c* release and apoptosis.

DNA damage was also extensive and contributed to JS-K's toxic potential, as indicated by the apparent protective effect of high OGG1 levels. The demonstrated increase in superoxide and probable increase in peroxynitrite probably caused this damage; previously we noted a correlation between basal superoxide levels and DNA damage in our panel of lung adenocarcinoma cell lines (Pacher et al., 2007; Romanowska et al., 2007). Oxidative DNA damage is predominantly repaired by BER, and OGG1 is responsible for most BER activity in humans. Both NO and peroxynitrite are capable of inhibiting OGG1 activity (Jaiswal et al., 2001) and may lead to further increase in DNA damage. Effects of DNA damage were p53-independent in H1703 cells; the mechanisms will need to be elucidated in further studies. Induction of apoptosis by NO or peroxynitrite donors has been described in other types of p53-deficient cells (Taylor et al., 2007).

Until now, the therapeutic effectiveness of NO generators against lung cancers has not seemed likely (Kashfi et al., 2002; Bentz et al., 2004, 2007; Chanvorachote et al., 2006). Results presented here show that, on the contrary, JS-K is empirically quite effective against a substantial percentage of lung cancer cell lines that are apparently vulnerable be-

cause of a combination of high ROS/RNS, low antioxidant PRX1, and low OGG1 DNA repair enzyme. PRX1 and OGG1 proteins could be easily quantified in tumor surgical or biopsy samples for selection of candidate lung cancer patients for JS-K therapy.

Authorship Contributions

Participated in research design: Maciag, Anderson, Saavedra, and Keefer.

Conducted experiments: Maciag, Chakrapani, Saavedra, Morris, and Holland.

Contributed new reagents or analytic tools: Kosak and Shami.

Performed data analysis: Maciag, Saavedra, and Anderson.

Wrote or contributed to the writing of the manuscript: Maciag, Anderson, and Keefer.

Other: Kosak and Shami reviewed and edited the manuscript.

References

Bagci EZ, Vodovotz Y, Billiar TR, Ermentrout B, and Bahar I (2008) Computational insights on the competing effects of nitric oxide in regulating apoptosis. *PloS One* **3:**e2249.

Bentz BG, Hammer ND, Milash B, Klein S, Burnett DM, Radosevich JA, and Haines GK 3rd (2007) The kinetics and redox state of nitric oxide determine the biological consequences in lung adenocarcinoma. *Tumour Biol* **28:**301–311.

Bentz BG, Hammer ND, Radosevich JA, and Haines GK 3rd (2004) Nitrosative stress induces DNA strand breaks but not caspase mediated apoptosis in a lung cancer cell line. *J Carcinog* **3:**16.

Bonavida B, Baritaki S, Huerta-Yepez S, Vega MI, Chatterjee D, and Yeung K (2008) Novel therapeutic applications of nitric oxide donors in cancer: roles in chemo- and immunosensitization to apoptosis and inhibition of metastases. *Nitric Oxide* **19:** 152–157.

Bonavida B, Khineche S, Huerta-Yepez S, and Garbán H (2006) Therapeutic potential of nitric oxide in cancer. *Drug Resist Updat* **9:**157–173.

Borutaite V and Brown GC (2003) Mitochondria in apoptosis of ischemic heart. *FEBS Lett* **541:**1–5.

Brookes PS, Bolaños JP, and Heales SJ (1999) The assumption that nitric oxide inhibits mitochondrial ATP synthesis is correct. *FEBS Lett* **446:**261–263.

Brown GC and Borutaite V (2006) Interactions between nitric oxide, oxygen, reactive oxygen species and reactive nitrogen species. *Biochem Soc Trans* **34:**953–956.

Carbone DP (2009) Profiles in variation: lung carcinogenesis. *Cancer Prev Res (Phila)* **2:**695–697.

Chakrapani H, Kalathur RC, Maciag AE, Citro ML, Ji X, Keefer LK, and Saavedra JE (2008) Synthesis, mechanistic studies, and antiproliferative activity of glutathione/glutathione *S*-transferase-activated nitric oxide prodrugs. *Bioorg Med Chem* **16:**9764–9771.

Chanvorachote P, Nimmannit U, Stehlik C, Wang L, Jiang BH, Ongpipatanakul B, and Rojanasakul Y (2006) Nitric oxide regulates cell sensitivity to cisplatin-induced apoptosis through S-nitrosylation and inhibition of Bcl-2 ubiquitination. *Cancer Res* **66:**6353–6360.

D'Alessio M, De Nicola M, Coppola S, Gualandi G, Pugliese L, Cerella C, Cristofanon S, Civitareale P, Ciriolo MR, Bergamaschi A, et al. (2005) Oxidative Bax dimerization promotes its translocation to mitochondria independently of apoptosis. *FASEB J* **19:**1504–1506.

Ferrer-Sueta G and Radi R (2009) Chemical biology of peroxynitrite: kinetics, diffusion, and radicals. *ACS Chem Biol* **4:**161–177.

Halliwell B and Whiteman M (2004) Measuring reactive species and oxidative damage in vivo and in cell culture: how should you do it and what do the results mean? *Br J Pharmacol* **142:**231–255.

Hofseth LJ, Hussain SP, Wogan GN, and Harris CC (2003) Nitric oxide in cancer and chemoprevention. *Free Radic Biol Med* **34:**955–968.

Huerta S, Chilka S, and Bonavida B (2008) Nitric oxide donors: novel cancer therapeutics (review). *Int J Oncol* **33:**909–927.

Jaiswal M, LaRusso NF, Nishioka N, Nakabeppu Y, and Gores GJ (2001) Human Ogg1, a protein involved in the repair of 8-oxoguanine, is inhibited by nitric oxide. *Cancer Res* **61:**6388–6393.

Jarry A, Charrier L, Bou-Hanna C, Devilder MC, Crussaire V, Denis MG, Vallette G, and Laboisse CL (2004) Position in cell cycle controls the sensitivity of colon cancer cells to nitric oxide-dependent programmed cell death. *Cancer Res* **64:**4227–4234.

Kashfi K, Ryann Y, Qiao LL, Williams JL, Chen J, del Soldato P, Traganos F, and Rigas B (2002) Nitric oxide-donating nonsteroidal anti-inflammatory drugs inhibit the growth of various cultured human cancer cells: evidence of a tissue type-independent effect. *J Pharmacol Exp Ther* **303:**1273–1282.

Kiziltepe T, Hideshima T, Ishitsuka K, Ocio EM, Raje N, Catley L, Li CQ, Trudel LJ, Yasui H, Vallet S, et al. (2007) JS-K, a GST-activated nitric oxide generator, induces DNA double-strand breaks, activates DNA damage response pathways, and induces apoptosis in vitro and in vivo in human multiple myeloma cells. *Blood* **110:**709–718.

Kröncke KD, Fehsel K, and Kolb-Bachofen V (1997) Nitric oxide: cytotoxicity versus cytoprotection–how, why, when, and where? *Nitric Oxide* **1:**107–120.

Li CQ and Wogan GN (2005) Nitric oxide as a modulator of apoptosis. *Cancer Lett* **226:**1–15.

MacMillan-Crow LA, Crow JP, and Thompson JA (1998) A peroxynitrite-mediated inactivation of manganese superoxide dismutase involves nitration and oxidation of critical tyrosine residues. *Biochemistry* **37:**1613–1622.

Pacher P, Beckman JS, and Liaudet L (2007) Nitric oxide and peroxynitrite in health and disease. *Physiol Rev* **87:**315–424.

Pelicano H, Carney D, and Huang P (2004) ROS stress in cancer cells and therapeutic implications. *Drug Resist Updat* **7:**97–110.

Phelps RM, Johnson BE, Ihde DC, Gazdar AF, Carbone DP, McClintock PR, Linnoila RI, Matthews MJ, Bunn PA Jr, Carney D, et al. (1996) NCI-Navy Medical Oncology Branch cell line data base. *J Cell Biochem Suppl* **24:**32–91.

Rauen U, Li T, Ioannidis I, and de Groot H (2007) Nitric oxide increases toxicity of hydrogen peroxide against rat liver endothelial cells and hepatocytes by inhibition of hydrogen peroxide degradation. *Am J Physiol Cell Physiol* **292:**C1440–C1449.

Ren Z, Kar S, Wang Z, Wang M, Saavedra JE, and Carr BI (2003) JS-K, a novel non-ionic diazeniumdiolate derivative, inhibits Hep 3B hepatoma cell growth and induces c-Jun phosphorylation via multiple MAP kinase pathways. *J Cell Physiol* **197:**426–434.

Romanowska M, Maciag A, Smith AL, Fields JR, Fornwald LW, Kikawa KD, Kasprzak KS, and Anderson LM (2007) DNA damage, superoxide, and mutant K-ras in human lung adenocarcinoma cells. *Free Radic Biol Med* **43:**1145–1155.

Royle JS, Ross JA, Ansell I, Bollina P, Tulloch DN, and Habib FK (2004) Nitric oxide donating nonsteroidal anti-inflammatory drugs induce apoptosis in human prostate cancer cell systems and human prostatic stroma via caspase-3. *J Urol* **172:** 338–344.

Saavedra JE, Srinivasan A, Bonifant CL, Chu J, Shanklin AP, Flippen-Anderson JL, Rice WG, Turpin JA, Davies KM, and Keefer LK (2001) The secondary amine/nitric oxide complex ion $R_2N[N(O)NO]^-$ as nucleophile and leaving group in S_NAr reactions. *J Org Chem* **66:**3090–3098.

Schiller JH, Harrington D, Belani CP, Langer C, Sandler A, Krook J, Zhu J, Johnson DH, and Eastern Cooperative Oncology Group (2002) Comparison of four chemotherapy regimens for advanced non-small-cell lung cancer. *N Engl J Med* **346:**92–98.

Shami PJ, Saavedra JE, Bonifant CL, Chu J, Udupi V, Malaviya S, Carr BI, Kar S, Wang M, Jia L, et al. (2006) Antitumor activity of JS-K [O^2-(2,4-dinitrophenyl) 1-[(4-ethoxycarbonyl)piperazin-1-yl]diazen-1-ium-1,2-diolate] and related O^2-aryl diazeniumdiolates in vitro and in vivo. *J Med Chem* **49:**4356–4366.

Shami PJ, Saavedra JE, Wang LY, Bonifant CL, Diwan BA, Singh SV, Gu Y, Fox SD, Buzard GS, Citro ML, et al. (2003) JS-K, a glutathione/glutathione *S*-transferase-activated nitric oxide donor of the diazeniumdiolate class with potent antineoplastic activity. *Mol Cancer Ther* **2:**409–417.

Shiva S, Brookes PS, Patel RP, Anderson PG, and Darley-Usmar VM (2001) Nitric oxide partitioning into mitochondrial membranes and the control of respiration at cytochrome *c* oxidase. *Proc Natl Acad Sci USA* **98:**7212–7217.

Taylor EL, Li JT, Tupper JC, Rossi AG, Winn RK, and Harlan JM (2007) GEA 3162, a peroxynitrite donor, induces Bcl-2-sensitive, p53-independent apoptosis in murine bone marrow cells. *Biochem Pharmacol* **74:**1039–1049.

Tomayko MM and Reynolds CP (1989) Determination of subcutaneous tumor size in athymic (nude) mice. *Cancer Chemother Pharmacol* **24:**148–154.

Trachootham D, Alexandre J, and Huang P (2009) Targeting cancer cells by ROS-mediated mechanisms: a radical therapeutic approach? *Nat Rev Drug Discov* **8:**579–591.

Voskoglou-Nomikos T, Pater JL, and Seymour L (2003) Clinical predictive value of the in vitro cell line, human xenograft, and mouse allograft preclinical cancer models. *Clin Cancer Res* **9:**4227–4239.

Yamakura F, Taka H, Fujimura T, and Murayama K (1998) Inactivation of human manganese-superoxide dismutase by peroxynitrite is caused by exclusive nitration of tyrosine 34 to 3-nitrotyrosine. *J Biol Chem* **273:**14085–14089.

Address correspondence to: Anna E. Maciag, SAIC-Frederick, Inc., National Cancer Institute, Bldg. 538, Rm. 206, Fort Detrick, Frederick, MD 21702. E-mail: maciaga@mail.nih.gov